

Fullerides of Pyrrolidine-Functionalized C₆₀

Yongping Sun,[†] Tatiana Drovetskaya,[†] Robert D. Bolskar,[†] Robert Bau,[†]
Peter D. W. Boyd,^{*,‡} and Christopher A. Reed^{*,†}

Departments of Chemistry, University of Southern California, Los Angeles, California 90089-0744, and
The University of Auckland, Private Bag 92019, Auckland 1, New Zealand

Received February 25, 1997[Ⓞ]

The spectral characteristics of the fulleride(1⁻) anions of pyrrolidine-functionalized C₆₀ derivatives have been investigated in order to assess the degree to which the parent C₆₀ moiety retains its distinctive redox and chromophoric properties upon functionalization. Such comparison data are necessary if C₆₀ is to fulfill its anticipated role as a versatile electron-accepting chromophore and a multielectron reservoir. Three systems have been investigated: a simple, monomeric, *N*-methylpyrrolidine derivative, **1**, a pyrrolidine-linked tetraphenylporphyrin/C₆₀ dyad, **2**, and a pair of bifullerenes, **3** and **4**, with adjacent and remote dispositions of the C₆₀ moieties, respectively. Near infrared spectra of the fulleride(1⁻) ions of these derivatives are notably similar to C₆₀¹⁻ with only small energy shifts of the band envelope. ¹H and ¹³C NMR data on **1**⁻ are consistent with unpaired spin density confined largely to the C₆₀ moiety rather than delocalized onto the pyrrolidine functionality. The EPR spectra of all of the pyrrolidine-functionalized fulleride(1⁻) species are characterized by sharp doublets ($\Delta H = 1-2$ G) and *g* values less than the free electron value. Unlike the EPR spectrum of C₆₀¹⁻, there is little temperature dependence of the line width. EPR evidence for ball-to-ball spin-spin interactions are observed in the fulleride of **3** but not in **4** or in the Cu^{II}C₆₀¹⁻ metalated porphyrin dyad. The X-ray crystal structure of the porphyrin-C₆₀ dyad **2** has been determined. It is the first X-ray structural characterization of a pyrrolidine-functionalized C₆₀ species and confirms that the azamethine ylide addition has occurred across a 6:6 ring juncture. The crystal packing of the dyad reveals an intermolecular interaction of the C₆₀ ball nestled in remarkably close approach to the porphyrin plane. The closest approach of a fullerene carbon atom to the mean plane of the porphyrin is ca. 2.75 Å. This interaction is notably similar to that envisaged for porphyrin-functionalized chromatographic supports used to separate fullerenes. A novel donor/acceptor relationship is proposed to account for this close interaction.

Introduction

As a redox-active chromophore, C₆₀ may eventually rival ferrocene and porphyrins in the versatility of its application to processes involving charge separation and storage. C₆₀ is functionalizable¹ and thus is readily tagged to itself,² to other chromophores,³ to polymers,⁴ and to biomolecules.⁵ It has strong electronic absorptions across the UV and visible portions of the electromagnetic spectrum and associated with this are distinctive photo-physical properties.⁶ C₆₀ has a unique redox chemistry in solution, adding up to six electrons with nearly equal spacings of potential in successive reductions.⁷ This electronegativity makes it an electron acceptor *par excel-*

lence, and hence, as a fulleride (C₆₀ⁿ⁻), it becomes a very attractive electron reservoir. Photoinduced charge separation in dyads with a C₆₀ moiety acting as the electron acceptor is currently receiving considerable attention,⁸ and an electroactive polymer based on (C₆₀O)_n has recently been described.^{4j} The hyperpolarizability of C₆₀¹⁻ is significantly greater than that of C₆₀, suggesting that fullerides rather than fullerenes will have superior nonlinear optical applications.⁹

A fundamental question underlying the application of C₆₀ to problems of charge separation and storage is the extent to which the redox properties of C₆₀ are retained when it is functionalized. How are its redox processes and reduction potentials affected?¹⁰ Are the reduction electrons and unpaired spin localized on the ball or are they delocalized onto the connecting functionality? How are electron transfer mechanisms affected by functionalization? Is the NIR region of the absorption spectrum as distinctive and useful for functionalized fullerides as it is for C₆₀ⁿ⁻ fullerides? Does the proximity of fullerene units lead to redox-activated ball-to-ball chemical reactivity? What is the nature of ball-to-ball spin coupling? These are some of the questions which must be answered before fullerenes can realize their full potential as unique and useful redox-active chromophores.

Our particular interest is centered on the electron reservoir possibilities of C₆₀. We have recently linked C₆₀ covalently to tetraphenylporphyrin^{3b} with the idea that fulleride substituents on a metalloporphyrin will promote multielectron reduction chemistry at an axial ligand binding site. We have chosen pyrrolidine derivatization of C₆₀ because, of the known methodologies for function-

[†] University of Southern California.

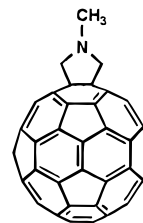
[‡] The University of Auckland.

[Ⓞ] Abstract published in *Advance ACS Abstracts*, May 1, 1997.

(1) (a) Diederich, F.; Thilgen, C. *Science* **1996**, *271*, 317–323. (b) Hirsch, A. *The Chemistry of the Fullerenes*; Georg Thieme Verlag: Stuttgart, 1994. (c) Taylor, R.; Walton, D. R. M. *Nature (London)* **1993**, *363*, 685–693.

(2) (a) Suzuki, T.; Li, Q.; Khemani, K. C.; Wudl, F. *J. Am. Chem. Soc.* **1992**, *114*, 7300–7301. (b) Belik, P.; Gügel, A.; Spickermann, J.; Müllen, K. *Angew. Chem., Int. Ed. Engl.* **1993**, *32*, 78–80. (c) Paquette, L. A.; Graham, R. J. *J. Org. Chem.* **1995**, *60*, 2958–2959. (d) Smith, A. B., III; Tokuyama, H.; Strongin, R. M.; Furst, G. T.; Romanow, W. J.; Chait, B. T.; Mirza, U. A.; Haller, I. *J. Am. Chem. Soc.* **1995**, *117*, 9359–9360. (e) Kraus, A.; Gügel, A.; Belik, P.; Walter, M.; Müllen, K. *Tetrahedron* **1995**, *51*, 9927–9940. (f) Lebedkin, S.; Ballenweg, S.; Gross, J.; Taylor, R.; Krätschmer, W. *Tetrahedron Lett.* **1995**, *36*, 4971–4974. (g) Osawa, S.; Osawa, E.; Harada, M. *J. Org. Chem.* **1996**, *61*, 257–265. (h) Timmerman, P.; Witschel, L. E.; Diederich, F.; Boudon, C.; Gisselbrecht, J.-P.; Gross, M. *Helv. Chim. Acta* **1996**, *79*, 6–20. (i) Paquette, L. A.; Trego, W. E. *J. Chem. Soc., Chem. Commun.* **1996**, 419–420. (j) Komatsu, K.; Takimoto, N.; Murata, Y.; Wan, T. S. M.; Wong, T. *Tetrahedron Lett.* **1996**, *37*, 6153–6156. (k) Irngartinger, H.; Weber, A. *Tetrahedron Lett.* **1996**, *37*, 4137–4140.

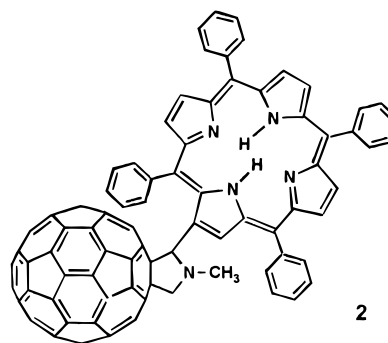
alizing C₆₀,¹ the addition of an azamethine ylide across a 6:6 ring juncture is synthetically versatile and the derivatized products have excellent thermal stability.¹¹ In addition, the reduction potentials of pyrrolidine-derivatized C₆₀ moieties typically remain fairly close to those of the corresponding reductions of free C₆₀.^{3f,10b} For example, Prato and co-workers^{3f} have shown that the first two reduction potentials of the *N*-methylpyrrolidine derivative **1** are cathodically shifted by 110 mV relative to that of C₆₀. A total of five reductions can be observed in the voltammetry of **1** with increasing differences in potential relative to that of C₆₀ as the negative charge increases. The retention of a similar number of voltametric reductions with relatively similar values for their reduction potentials is the basis of the general expecta-



1

tion that C₆₀ retains its fulleride-like properties in its reduced derivatives.¹⁰ In this paper, we examine this expectation in more detail by isolating the fulleride(1⁻) ion of **1** for NMR, EPR and NIR characterization.

As a prototype for studying spin-spin coupling phenomena, we have put a paramagnetic metal ion (Cu²⁺) into the porphyrin-C₆₀ dyad **2** and used EPR and NIR spectroscopy to probe the interaction between copper(II) and the appended fulleride(1⁻) radical anion.



2

We also report the synthesis and characterization of bifullerenes **3** and **4**, linked *meta* and *para* to benzene via pyrrolidine amides. Molecular modeling suggests that the C₆₀ moieties in **3** are held in van der Waals contact whereas those in **4** are held remote from each other.

The idea behind the synthesis of **3** was to probe potential ball-to-ball chemical and spectroscopic interactions. The possibility of ball-to-ball addition chemistry must be considered in light of the polymer¹² and dimer¹³ phases of KC₆₀ and RbC₆₀. We also wanted to investigate the EPR spectral characteristics of the anions of **1**, **3**, and **4** to see if they would shed light on the origin of unexplained peaks in the EPR spectra of C₆₀ⁿ⁻ fullerides.

(3) Porphyrins: (a) Liddell, P. A.; Sumida, J. P.; MacPherson, A. N.; Noss, L.; Seely, G. R.; Clark, K. N.; Moore, A. L.; Moore, T. A.; Gust, D. *Photochem. Photobiol.* **1994**, *60*, 537–541. (b) Drovetskaya, T.; Reed, C. A.; Boyd, P. D. W. *Tetrahedron Lett.* **1995**, *36*, 7971–7974. (c) Imahori, H.; Hagiwara, K.; Akiyama, T.; Taniguchi, S.; Okada, T.; Sakata, Y. *Chem. Lett.* **1995**, 265–266. (d) Imahori, H.; Sakata, Y. *Chem. Lett.* **1996**, 199–200. (e) Ranasinghe, M. G.; Oliver, A. M.; Rothenfluh, D. F.; Salek, A.; Paddon-Row, M. N. *Tetrahedron Lett.* **1996**, *37*, 4997–4800. Ferrocene: (f) Maggini, M.; Karlsson, A.; Scorrano, G.; Sandomà, G.; Farnia, G.; Prato, M. *J. Chem. Soc., Chem. Commun.* **1994**, 589–590. (g) Prato, M.; Maggini, M.; Giaometti, C.; Scorrano, G.; Sandomà, G.; Farnia, G. *Tetrahedron* **1996**, *52*, 5221–5234. Phthalocyanine: (h) Linszen, T. G.; Dürr, K.; Hanack, M.; Hirsch, A. *J. Chem. Soc., Chem. Commun.* **1995**, 103–104. Tris(bipyridine)ruthenium: (i) Maggini, M.; Donò, A.; Scorrano, G.; Prato, M. *J. Chem. Soc., Chem. Commun.* **1995**, 845–846. (j) Sariciftci, N. S.; Wudl, F.; Heeger, A. J.; Maggini, M.; Scorrano, G.; Prato, M.; Bourassa, J.; Ford, P. C. *Chem. Phys. Lett.* **1995**, *247*, 510–514. (k) Armspach, D.; Constable, E. C.; Diederich, F.; Housecroft, C. E.; Nierengarten, J.-F. *Chem. Commun.* **1996**, 2009–2010. Electron-rich moieties: (l) Khan, S. I.; Oliver, A. M.; Paddon-Row, M. N.; Rubin, Y. *J. Am. Chem. Soc.* **1993**, *115*, 4919–4920. (m) Diederich, F.; Jonas, U.; Gramlich, V.; Herrmann, A.; Ringsdorf, H.; Thilgen, C. *Helv. Chim. Acta* **1993**, *76*, 2445–2453. (n) Williams, R. M.; Zwier, J. M.; Verhoeven, J. W. *J. Am. Chem. Soc.* **1995**, *117*, 4093–4099. (o) Imahori, H.; Cardoso, S.; Tatman, D.; Lin, S.; Macpherson, A. N.; Noss, L.; Seely, G. R.; Sereno, L.; Chessa de Silber, J.; Moore, T. A.; Moore, A. L.; Gust, D. *Photochem. Photobiol.* **1995**, *62*, 1009–1014. (p) Diederich, F.; Dietrich-Buchecker, C.; Nierengarten, J.-F.; Sauvage, J.-P. *J. Chem. Soc., Chem. Commun.* **1995**, 781–782. (q) Warrenner, R. N.; Eelsey, G. M.; Houghton, M. A. *Ibid.* **1995**, 1417–1418. (r) Murata, Y.; Komatsu, K.; Wan, T. S. M. *Tetrahedron Lett.* **1996**, *37*, 7061–7064. (s) Fernandez-Paniagua, U. M.; Illescas, B. M.; Martin, N.; Scoane, C. *J. Chem. Soc., Perkins Trans. 1* **1996**, 1077–1079. (t) Lawson, J. M.; Oliver, A. M.; Rothenfluh, D. F.; Ellis, G. A.; Ranasinghe, M. G.; Khan, S. I.; Franz, A. G.; Ganapathi, P. S.; Shephard, M. J.; Paddon-Row, M. N.; Rubin, Y. *J. Org. Chem.* **1996**, *61*, 5032–5054. (u) Williams, R. M.; Koeberg, M.; Lawson, J. M.; An, Y.-Z.; Rubin, Y.; Paddon-Row, M. N.; Verhoeven, J. W. *J. Org. Chem.* **1996**, *61*, 5055–5062. (v) Martin, N.; Sanchez, L.; Seoane, C.; Andreu, R.; Garin, J.; Orduna, J. *Tetrahedron Lett.* **1996**, *37*, 5979–5982. Electron-poor moieties: (w) Shu, L. H.; Wang, G. W.; Wu, S. H.; Wu, H. M. *Ibid.* **1995**, 367–368. (x) Ohno, T.; Martin, N.; Knight, B.; Wudl, F.; Suzuki, T.; Yu, H. *J. Org. Chem.* **1996**, *61*, 1306–1309. (y) Iyoda, M.; Sasaki, S.; Sultana, F.; Yoshida, M.; Kuwatani, Y.; Nagase, S. *Tetrahedron Lett.* **1996**, *37*, 7987–7988.

(4) (a) Loy, D. A.; Assink, R. A. *J. Am. Chem. Soc.* **1992**, *114*, 3977–3978. (b) Sariciftci, N. S.; Smilowitz, L.; Heeger, A. J.; Wudl, F. *Science* **1992**, *258*, 1474–1476. (c) Shi, S.; Khemani, K. C.; Li, Q. C.; Wudl, F. *J. Am. Chem. Soc.* **1992**, *114*, 10656–10657. (d) Samulski, E. T.; DeSimone, J. M.; Hunt, M. O., Jr.; Menciloglu, Y. Z.; Jarnagin, R. C.; York, G. A.; Labat, K. B.; Wang, H. *Chem. Mater.* **1992**, *4*, 1153–1157. (e) Geckeler, K. E.; Hirsch, A. *J. Am. Chem. Soc.* **1993**, *115*, 3850–3851. (f) Patil, A. O.; Schrivve, G. W.; Carstensen, B.; Lundberg, R. D. *Polym. Bull.* **1993**, *30*, 187–190. (g) Berrada, M.; Hashimoto, Y.; Miyata, S. *Chem. Mater.* **1994**, *6*, 2023–2025. (h) Thomas, R. N. *J. Polym. Sci. A* **1994**, *32*, 2727–2737. (i) Geckeler, K. E. *Trends Polym. Sci.* **1994**, *2*, 355–360. (j) Fedurco, M.; Costa, D. A.; Balch, A. L.; Fawcett, W. R. *Angew. Chem., Int. Ed. Engl.* **1995**, *34*, 194–196. (k) Camp, A. G.; Lary, A.; Ford, W. T. *Macromolecules* **1995**, *28*, 7959–7961. (l) Zhang, N.; Schrickler, S. R.; Wudl, F. *Chem. Mater.* **1995**, *7*, 441–442. (m) Cao, T.; Webber, S. E. *Macromolecules* **1995**, *28*, 3741–3743. (n) Bunker, C. E.; Lawson, G. E.; Sun, Y. P. *Macromolecules* **1995**, *28*, 3744–3746. (o) Chen, Y.; Cai, R.-F.; Huang, Z.-E.; Bai, X.; Chen, S.-M.; Yan, X. M. *Solid State Commun.* **1996**, *97*, 239–242. (p) Chen, Y.; Huang, Z.-E.; Cai, R.-F. *J. Polym. Sci. B* **1996**, *34*, 631–640. (q) Liu, B.; Bunker, C. E.; Sun, Y.-P. *Chem. Commun.* **1996**, 1241–1242. (r) Cloutet, E.; Gnanou, Y.; Fillaut, J.-L.; Astruc, D. *Chem. Commun.* **1996**, 1565–1566.

(5) (a) Boutorine, A. S.; Tokuyama, H.; Takasugi, M.; Isobe, H.; Nakamura, E.; Hélène, C. *Angew. Chem., Int. Ed. Engl.* **1994**, *33*, 2462–2465. (b) Toniolo, C.; Bianco, A.; Maggini, M.; Scorrano, G.; Prato, M.; Marastoni, M.; Tomatis, R.; Spisani, S.; Palù, G.; Blair, E. D. *J. Med. Chem.* **1994**, *37*, 4558–4562. (c) Jensen, A. W.; Wilson, S. R.; Schuster, D. I. *Bioorg. Med. Chem.* In press.

(6) Foote, C. S. in *Top. Curr. Chem.* **1994**, *169*, 347–363. (7) (a) Xie, Q.; Pérez-Cordero, E.; Echegoyen, L. *J. Am. Chem. Soc.* **1992**, *114*, 3978–3980. (b) Ohsawa, Y.; Saji, T. *J. Chem. Soc., Chem. Commun.* **1992**, 781–782.

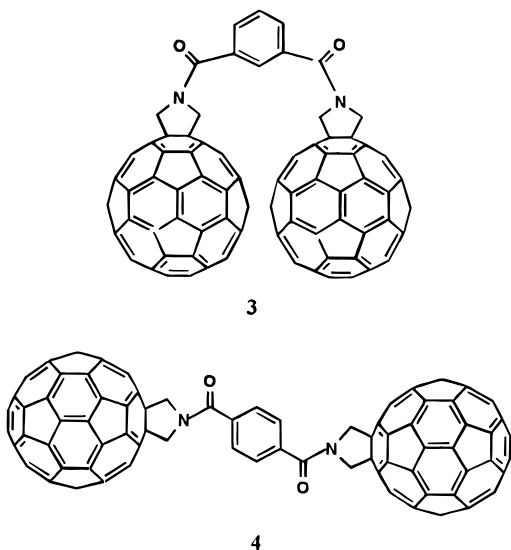
(8) See refs 3a,c,j,m,t, and Kuciauski, D.; Lin, S.; Seely, G. R.; Moore, A. L.; Moore, T. A.; Gust, D.; Drovetskaya, T.; Reed, C. A.; Boyd, P. D. W. *J. Phys. Chem.* **1996**, *100*, 15926–15932.

(9) Lascola, R.; Wright, J. C. *Chem. Phys. Lett.* In press. (10) (a) Wudl, F. *Acc. Chem. Res.* **1992**, *25*, 157–161. (b) Suzuki, T.; Muruyama, Y.; Akasaka, T.; Ando, W.; Kobayashi, K.; Nagase, S. *J. Am. Chem. Soc.* **1994**, *116*, 1359–1363.

(11) Maggini, M.; Scorrano, G.; Prato, M. *J. Am. Chem. Soc.* **1993**, *115*, 9798–9799.

(12) Pekker, S.; Jánossy, A.; Mihaly, L.; Chauvet, O.; Carrard, M.; Forró, L. *Science* **1994**, *265*, 1077–1078.

(13) Zhu, Q.; Cox, D. E.; Fischer, J. E. *Phys. Rev. B* **1995**, *51*, 3966–3969.



The existence of a “spike” in the C_{60}^{1-} spectrum and various triplets in the C_{60}^{2-} spectrum have no wholly satisfactory explanation,¹⁴ and we are considering the possibility that they might arise from $(C_{60})_2^{1-}$ and $(C_{60})_2^{2-}$, respectively, or from derivatized impurities similar to those of **1**.

Experimental Section

All manipulations of air-sensitive compounds were carried out in an inert atmosphere in a Vacuum Atmospheres drybox under helium (H_2O , $O_2 < 1$ ppm). C_{60} was purchased from MER Corp. and used without any further purification. **1** and $C_{60}(CH_2)_2NCPH_3$ were prepared by the published method,¹¹ and all other chemicals were purchased from Aldrich. Solvents were purified and dried by being heated under reflux overnight with the agent indicated below, distilled or vacuum distilled both outside and inside the glovebox, passed through a short column of activated neutral alumina, and stored over 3A molecular sieves. Pyridine was distilled from sodium metal, toluene from sodium benzophenone ketyl, benzonitrile and *o*-dichlorobenzene from a small piece of sodium metal, and dimethyl sulfoxide (DMSO) from CaH_2 . Deuterated DMSO was dried by passage through activated alumina and stored over 3A molecular sieves. Deuterated nitrobenzene was first vacuum distilled and then dried similarly.

EPR spectra were recorded in frozen solution near liquid He temperatures on a Bruker ER 200D-SRC spectrometer equipped with an Oxford Instruments ESR 900 cryostat, and g values were determined by calibration to DPPH powder. Vis-NIR spectra were recorded on an Ocean Optics spectrometer. NMR spectra were recorded at room temperature on a Bruker AC-250, AM-360, or AMX-500-MHz spectrometer, and the chemical shifts were calibrated against internal solvent or a sealed acetone- d_6 capillary. Reduction potentials for **2**, **3**, and **4** were obtained as previously described.⁸

[Cp₂Co⁺][1¹⁻]. **1** (25 mg, 0.032 mmol) was stirred with cobaltocene (6.2 mg, 0.033 mmol) in benzonitrile (2 mL) for several hours. Half of the solvent was removed under vacuum, and toluene was added to effect precipitation of the product. This solid was filtered off, washed with toluene several times, and pumped to dryness (30 mg, 97%): ¹H NMR (DMSO- d_6) δ 1.4 (br, 4H, CH₂), 4.1 (br, 3H, CH₃), 5.8 (10H, Cp₂Co⁺); ¹³C NMR (DMSO- d_6) δ 85.1 (Cp₂Co⁺), 187 (C₆₀-pyrrolidine anion);

NIR (benzonitrile) $\lambda_{max}(\epsilon) = 1002 (7.8 \times 10^3)$, 882 (3.6×10^3), 780 (3.0×10^3) nm.

Bifullerene 3. To a suspension of $C_{60}(CH_2)_2NCPH_3$ (150 mg, 0.149 mmol) in CH_2Cl_2 (30 mL) was added triflic acid (0.4 mL), and the mixture was stirred for 2 h. After the solution volume was reduced, Et₂O (10 mL) was added and the precipitate was centrifuged and washed several times with Et₂O, benzene, and Et₂O again. The brownish solid was pumped to dryness, taken into the glovebox, and suspended in *o*-dichlorobenzene (15 mL). To this were added 1,3-C₆H₄-(COCl)₂ (15.1 mg, 0.0744 mmol) and pyridine (2.3 mL), and after 8 h of stirring, the reaction mixture was removed from the glovebox and the product was filtered off and washed with methanol and hexane several times (119 mg, 96%): ¹H NMR (CS₂, CDCl₃) δ 5.56 (br, 8 H, CH₂), 7.80 (t, $J = 7.7$ Hz, 1H), 8.10 (dd, $J = 7.6$ Hz, $J = 1.6$ Hz, 2H), 8.36 (t, $J = 1.6$ Hz, 1H); ¹³C NMR (CS₂, acetone- d_6 as insert) δ phenyl ring 129.0, 129.4, 131.3, 135.6; fullerene peaks 136.1, 140.5, 142.1, 142.3, 142.4, 142.9, 143.3, 144.6, 145.5, 145.6, 145.7, 145.9, 146.3, 146.5, 147.5, 153.3; C=O 168.2.

Bifullerene 4. This was prepared in a similar manner to **3** using 1,4-C₆H₄(COCl)₂. **4**: ¹H NMR (CS₂, acetone- d_6 as insert) δ 4.84 (br, 8H, CH₂), 7.32 (s, 4H); ¹³C NMR (CS₂, acetone- d_6 as insert) δ phenyl ring 129.15, 137.61; fullerene peaks 136.1, 140.5, 142.2, 142.3, 142.4, 142.9, 143.3, 144.7, 145.5, 145.6, 145.7, 145.9, 146.3, 146.5, 147.5, 153.3.

EPR Sample of 3¹⁻. A deficit of reducing agent was used to ensure that no reduction to the (2-) state occurred. **3** (5.0 mg, 3.0×10^{-3} mmol) and 2.5×10^{-3} M cobaltocene PhCN solution (0.50 mL, 1.3×10^{-3} mmol) were mixed in PhCN (2 mL) and stirred for several hours. The suspension was filtered, and the supernatant was sealed in an EPR tube.

EPR Sample of 3²⁻. This was prepared in a similar manner using 0.275 mL of the cobaltocene solution (6.88×10^{-3} mmol). EPR samples of **4¹⁻** and **4²⁻** were prepared in an identical manner.

Copper(II)-Metalated 2. This was prepared in the same manner as for **2^{3b}** except that Cu(β -CHO-TPP) replaced Ni(β -CHO-TPP). Copper(II)-metalated **2¹⁻** was prepared by addition of cobaltocene to a solution of copper(II)-metalated **2** in *o*-dichlorobenzene.

X-ray Structure of 2. Well-shaped black prisms of **2^{3b}** suitable for X-ray diffraction were obtained by slow diffusion of hexane into a solution of **2** in $CHCl_3/CS_2(1:1)$.

Compound **2** (C₁₀₈H₃₆Cl₃N₅, $M_r = 1509.77$) crystallized in the monoclinic space group $P2(1)/n$ with cell dimensions of $a = 14.2520(10)$ Å, $b = 22.412(2)$ Å, $c = 21.238(2)$ Å, $\beta = 91.760(10)$, $V = 6780.6(10)$ Å³, $Z = 4$. Data were collected at -110 °C on a SIEMENS P4/RA diffractometer using graphite-monochromated Cu K α radiation ($\lambda = 1.54178$ Å) to a maximum $2\theta = 102.5^\circ$. The structure was solved by direct methods (SHELXTL IRIS) and refined against F^2 (SHELX93) yielding $R_1 = 0.0801$ for 5605 reflections with $I > 2\sigma(I)$ and $R_1 = 0.0967$ for all data (7301 independent reflections, $R_{int} = 0.0349$).

Refinement showed that the position of the C₆₀-*N*-methylpyrrolidine part of the molecule could be resolved into two orientations with major/minor relative populations of 0.58/0.42. The same was true for the $CHCl_3$ solvate molecule which is located near the pyrrolidine N atom. Additionally, the phenyl groups of the TPP fragment showed orientational disorder and were resolved into three or two orientational sites each. During the refinement it became obvious from the observation of excess electron density at the center of the porphyrin that it was partially metalated. Final refinement included 19% cobalt occupation. This must have arisen during recrystallization whereby traces of the cobalt-metalated species, a residual from incomplete demetalation in the synthesis reaction,^{3b,15} were concentrated in the single crystal.³⁷

Results and Discussion

Properties of the *N*-Methylfulleropyrrolidine(1-) Anion, 1¹⁻. Reduction of **1** to its fulleride(1-) ion was

(14) (a) Stinchcombe, J.; Pénicaud, A.; Bhyrappa, P.; Boyd, P. D. W.; Reed, C. A. *J. Am. Chem. Soc.* **1993**, *115*, 5212–5217. (b) Khaled, M. M.; Carlin, R. T.; Trulove, P. C.; Eaton, G. R.; Eaton, S. S. *J. Am. Chem. Soc.* **1994**, *116*, 3465–3474. (c) Boyd, P. D. W.; Bhyrappa, P.; Paul, P.; Stinchcombe, J.; Bolskar, R.; Sun, Y.; Reed, C. A. *J. Am. Chem. Soc.* **1995**, *117*, 2907–2914. (d) Brezová, V.; Stasko, A.; Rapta, P.; Domschke, G.; Bartl, A.; Dunsch, L. *J. Phys. Chem.* **1995**, *99*, 16234–16241 and references within these papers.

(15) Ponomarev, G. V.; Maravin, G. B. *Chem. Heterocycl. Compd.* **1982**, *18*, 50–55.

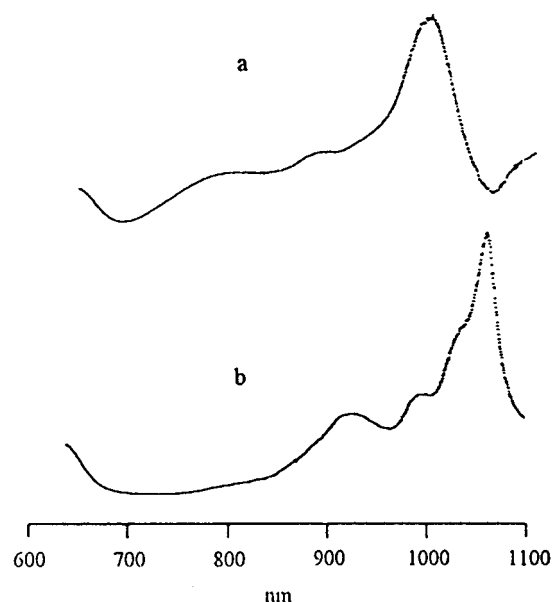


Figure 1. Comparison of NIR spectra in benzonitrile solution: (a) the *N*-methylpyrrolidine-derivatized fulleride **1**¹⁻, (b) C₆₀¹⁻ as CoCp₂⁺ salts.

readily achieved with cobaltocene or with the sodium/crown ether (1 equiv) method as developed earlier for C₆₀.^{14a} Unlike C₆₀, where the cobaltocene/cobaltocenium redox potential is sufficiently negative that further reduction can occur to give some C₆₀²⁻, the pyrrolidine-functionalized C₆₀ species are reduced selectively to the monoanion by cobaltocene. This reflects the 110 mV more negative reduction potential of **1** relative to that of C₆₀.¹¹

Near infrared (NIR) spectroscopy offers distinctive fingerprints for fullerides because the LUMO/LUMO+1 energy gap of C₆₀ is about 1 eV.¹⁶ Notably, the distinctive fingerprint of C₆₀¹⁻ is retained in **1**¹⁻ although, as shown in Figure 1, there is a small blue shift of λ_{max} (by ca. 70 nm). Similar observations have been reported in a Diels–Alder adduct.¹⁷ These findings are consistent with a LUMO electronic structure that has only minor perturbations from C₆₀. It would be premature to suggest assignments for the observed transitions given that the NIR spectrum of C₆₀¹⁻ is incompletely understood.¹⁸

We next explored the locale of electron spin density in **1**¹⁻ as reflected in the response of its NMR active nuclei to the presence of paramagnetism. The ¹H NMR spectrum of [CoCp₂][**1**] in dimethyl-*d*₆ sulfoxide solution is shown in Figure 2. The CoCp₂⁺ resonance appears as a singlet at 5.8 ppm. The three *N*-CH₃ protons on the pyrrolidine appear as a broad singlet at 4.1 ppm, somewhat downfield shifted from their diamagnetic position at 3.00. The four methylene protons appear as a broad resonance at 1.4 ppm, upfield shifted from their diamagnetic position at 4.39 ppm. The assignments were consistent with integration of the areas under each peak and were verified by comparison to the corresponding

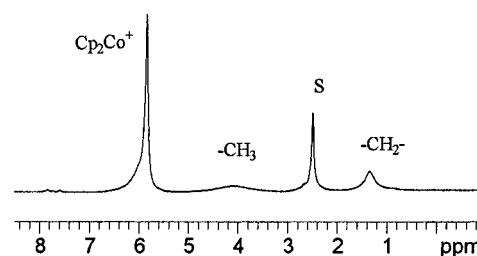


Figure 2. ¹H NMR spectrum (DMSO-*d*₆) of **1**¹⁻ (s denotes peak due to solvent).

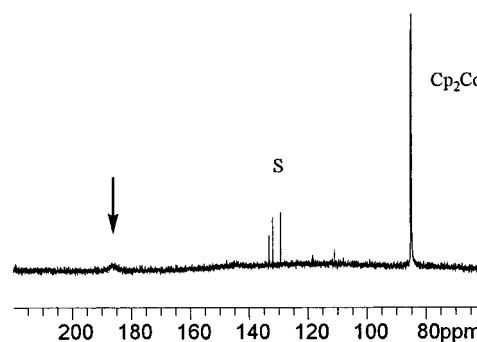


Figure 3. ¹³C NMR spectrum (DMSO-*d*₆) of **1**¹⁻ (s denotes peaks due to a trace of benzonitrile).

N-trityl species whose methylene protons shift from 4.17 to 1.2 ppm upon reduction (in nitrobenzene-*d*₅). The direction and magnitude of these shifts can be understood by considering the nature of the SOMO (singly occupied molecular orbital)—see below.

The ¹³C NMR spectrum of [CoCp₂][**1**] shows only two detectable peaks, that of the cation at 85.1 ppm and a broad (ca. 10 ppm) fulleride peak centered at 187 ppm (see Figure 3). The close similarity with that of unfunctionalized C₆₀¹⁻ whose 2–3 ppm wide signal appears centered at 186 ppm is notable.^{14c} In diamagnetic **1**, the sp² buckyball ¹³C signals span the range 136–154 ppm, although the majority cluster around 143 ± 3 ppm.¹¹ Upon reduction to paramagnetic **1**¹⁻, they experience almost precisely the same average downfield shift and broadening as does C₆₀. This is compelling evidence for the view that the unpaired electron in **1**¹⁻ is delocalized over the buckyball in much the same way as it is in C₆₀¹⁻ and that the average spin density seen by the majority of the sp² carbon atoms is the same. The sp³ carbon atoms on the buckyball, as well as those on the pyrrolidine ring, are not observed, presumably due to the combination of low relative abundance and paramagnetic broadening.

The third experimental technique we have used to probe the electronic nature of pyrrolidine-functionalized fullerides is EPR spectroscopy. Typical spectra arising from **1**¹⁻ are shown in Figure 4. Narrow isotropic doublets are seen at all temperatures although there are hints of anisotropy at the lowest temperatures (ca. 4 K). There is a detectable effect of the cation, cobaltocenium versus Na(crown)⁺, but this is much less dramatic than that seen in C₆₀¹⁻.^{14a} Apparently, the inherently lower symmetry and the presence of the addends in these functionalized fullerides makes them much less sensitive to the effects of ion pairing. The *g* values are, however, quite similar to those of C₆₀¹⁻ and, although a little higher, are diagnostically below the free electron value. The greatest difference between the EPR spectrum of

(16) (a) Kato, T.; Kodama, T.; Oyama, M.; Okazaki, S.; Shida, T.; Nakagawa, T.; Matsui, Y.; Suzuki, S.; Shiromaru, H.; Yamauchi, K.; Achiba, Y. *Chem. Phys. Lett.* **1991**, *186*, 35–39. (b) Lawson, D. R.; Feldheim, D. L.; Foss, C. A.; Dorhout, P. K.; Elliott, C. M.; Martin, C. R.; Parkinson, B. *J. Electrochem. Soc.* **1992**, *139*, L68–71.

(17) Baumgarten, M.; Gherghel, L. *Progress in Fullerene Research*; World Scientific: Singapore, 1994; pp 384–388.

(18) (a) Kondo, H.; Momose, T.; Shida, T. *Chem. Phys. Lett.* **1995**, *237*, 111–114. (b) Bolskar, R. D.; Gallagher, S. H.; Armstrong, R. S.; Lay, P. A.; Reed, C. A. *Chem. Phys. Lett.* **1995**, *247*, 57–62.

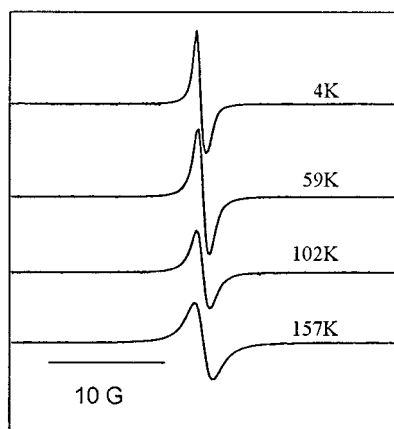


Figure 4. Typical EPR spectra of the fulleride(1⁻) ion of a pyrrolidine-functionalized C₆₀, **1**¹⁻, in frozen benzonitrile ($g = 2.0006$).

C₆₀¹⁻ and its derivatives is the temperature dependence of the line width.¹⁷ In C₆₀¹⁻, the line width increases from a few gauss at low temperatures to tens of gauss at room temperature.^{14a} A dynamic Jahn–Teller effect (pseudorotation) and lifetime broadening from thermal population of a low-lying excited state are among the proposals to account for this. By contrast, the line width of **1**¹⁻ increases by no more than 1–2 G over a similar temperature range. Obviously, the functionalization of C₆₀ eliminates the possibility of significant pseudorotation (and of real rotation in frozen solution). It may also separate the ground state further from the first excited state inasmuch as permanent functionalization may remove the (t_{1u})¹ triple degeneracy of C₆₀¹⁻ more effectively than a Jahn–Teller distortion. Finally, we note that there is no evidence for hyperfine coupling to N or H. This is consistent with very low spin density on the pyrrolidine functionality.

The overall close spectroscopic similarity of **1**¹⁻ to C₆₀¹⁻, particularly with techniques that probe unpaired electron spin density, has led us to seek calculational support for the emerging picture of spin delocalized over the buckyball but not onto the pyrrolidine functionality. Semi-empirical molecular orbital calculations of the electronic and molecular structure^{19,20} of the monoanion using the PM3 method show that the SOMO is principally localized on the fullerene cage. Examination of spin density maps indicates that the majority of the unpaired electron is localized on the fullerene carbon atoms. Figure 5 shows a surface representation of the LUMO for the neutral molecule at the contour level of 0.001 e au⁻³. It shows that only very small components of this orbital are delocalized from the fullerene cage. The nodal sequence of this molecular orbital in the pyrrolidine ring leads to an orthogonality of the carbon p orbital with respect to the methylene protons and delocalization of the orbital onto the methyl protons. The proton isotropic hyperfine coupling constants calculated from the observed shifts are -0.042 and +0.014 G for the methylene and *N*-methyl protons, respectively. These coupling constants are in keeping with the calculated form of the SOMO. Spin density at the methylene protons arises from a spin polarization mechanism whilst that at the *N*-methyl protons arises from direct delocalization, leading to a

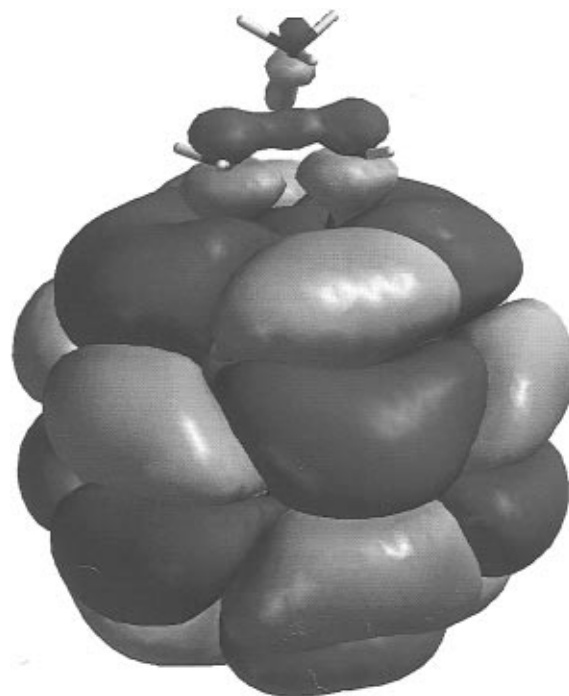


Figure 5. Contour surface of the LUMO of **1** calculated from the PM3 wave function at a value of 0.002 e au⁻³.

contact interaction. An approximate estimate of the spin density assuming a McConnell type relationship gives a value of 0.001–0.002 (0.1–0.2%) at the methylene carbon atoms. This suggests an upper limit of 0.5% for the delocalization of the unpaired electron from the fullerene cage onto the *N*-methylpyrrolidine ring.

X-ray Structure of the Porphyrin–C₆₀ Dyad, 2. The synthesis, the ground state perturbation of the electronic spectrum of the porphyrin by the C₆₀ substituent, the redox potentials, and the photoinduced electron transfer of **2** have been reported.^{3b,8} We now report on its crystal structure as a chloroform solvate. We have been fortunate in growing X-ray diffraction quality crystals, but as often seems to be the case with C₆₀ structures,²¹ there is crystallographic disorder which, in the present case, defeats the goal of obtaining useful molecular bond lengths and angles from the data. Nevertheless, the disposition of the porphyrin and C₆₀ moieties, both intra- and intermolecularly, are well-resolved, as are the modes of linkage.

Perhaps the most interesting feature of the structure is the intermolecular packing relationship of C₆₀ to the porphyrin. Figure 6 illustrates the pairwise, ball-on-hand manner in which the buckyball makes intermolecular contact with the porphyrin. There are two crystallographically distinct contacts. The distances of the closest C₆₀ carbon atoms to the mean plane of the 16-atom inner core of the porphyrin ring are very short: 2.78 Å to one ring and 2.79 Å to the other. (The corresponding distances in the minor orientation, which arises from crystallographic disorder, are 2.75 and 2.70 Å.) The shortness of these distances is apparent when comparisons are made to the inter-layer separation of graphite (3.35 Å), to interfacial porphyrin/porphyrin separations (>3.2 Å),²² to the separations of C₆₀ from

(19) Calculations were performed using Spartan version 4.1, Wavefunction Inc., Irvine, CA 92715.

(20) Stewart, J. J. P. *J. Comput. Chem.* **1989**, *10*, 209–220.

(21) Balch, A. L.; Lee, J. W.; Noll, B. C.; Olmstead, M. M. *J. Chem. Soc., Chem. Commun.* **1993**, 56–58.

(22) Scheidt, W. R.; Lee, Y. J. *Struct. Bonding (Berlin)* **1987**, *64*, 1–70.

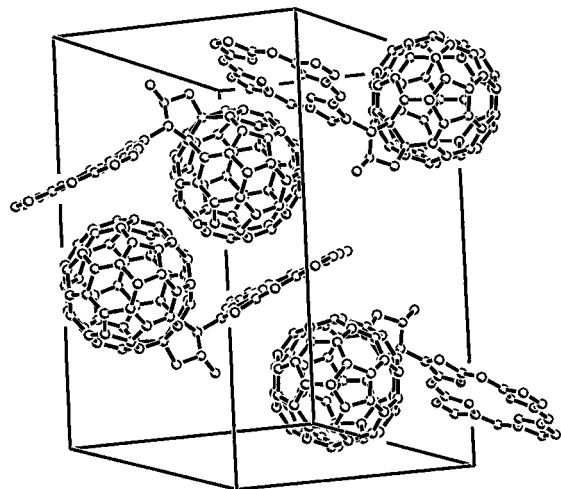


Figure 6. Perspective drawing of the unit cell packing in the crystal structure of **2** (major orientation) showing close ball/porphyrin intermolecular interactions. Phenyl substituents on the porphyrins and the chloroform solvate are omitted for clarity.

arene rings in various X-ray structures (ca. 3.0–3.5 Å),^{21,23–25} and to ball-to-ball separations in C₆₀ and its derivatives (>3.2 Å).^{21,23,24} This suggests that the usual and expected π/π interaction is substantially augmented by a strong donor/acceptor interaction. There is a close structural analogy to the interaction of arenes with the (tetraphenylporphyrinato)iron(III) cation, Fe(TPP)⁺. In the crystal structure of [Fe(TPP)·*p*-xylene]⁺, two arene carbon atoms approach to within 2.89 Å of the porphyrin plane.²⁶ In the sterically less-hindered toluene analog, the closest approach is even shorter (2.71 Å).²⁷ With its curved surface, C₆₀ is sterically suited to a similarly close approach and the electroneutrality of the porphyrin in **2** vis-à-vis the cationic nature of Fe(TPP)⁺ serves only to emphasize the closeness of the approach. In contrast to the usual view of C₆₀ as an acceptor, the sense of the donor/acceptor relationship might be with C₆₀ as the donor and the porphyrin (or metalloporphyrin)²⁸ as the acceptor. Figure 7 shows plane projections of the closest carbon atoms of C₆₀ onto the porphyrin planes for the two contacts in their major orientations. In one, the C₆₀ carbon atom closest to the porphyrin plane is also the carbon atom closest to the center of the porphyrin. In

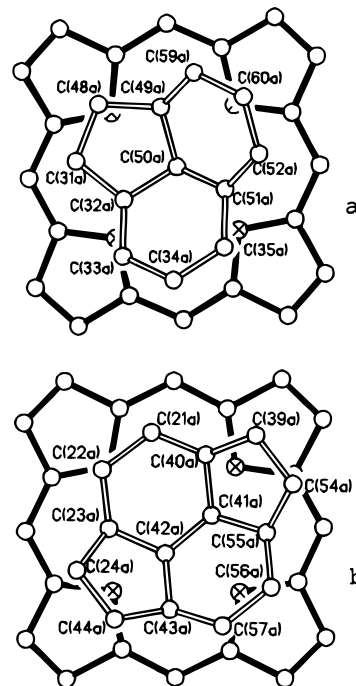


Figure 7. Plane projections of portions of the C₆₀ moieties (open bonds) onto the porphyrin cores (filled bonds) for the two intermolecular contacts of the major orientation. Closest approaches to the porphyrin planes are (a) C(41a) 2.79 Å, C(42a) 2.82 Å, C(40a) 3.02 Å, C(23a) 3.06 Å, C(22a) 3.28 Å, (b) C(50a) 2.78 Å, C(32a) 2.97 Å, C(49a) 3.00 Å, C(51a) 3.19 Å.

the other, it is the second closest atom by a mere 0.07 Å. This centering of the buckyball over the porphyrin is consistent with the proposed donor/acceptor relationship because the two hydrogen atoms (or a metal)²⁸ at the center of the porphyrin are the locus of acidity in this otherwise relatively electron-rich macrocycle. It could be argued that the centering is simply the result of crystal packing. However, the closeness of the approach of the C₆₀ moiety to the porphyrin suggests there is a strong electronic effect as well.

With C₆₀ as the donor in this interaction, one might expect that the more electron-rich bonds of the buckyball would be closest to the porphyrin, i.e., the more electron rich “double” bonds at 6:6 ring junctures might interact with the porphyrin in preference to the less electron-rich “single” bonds at 5:6 ring junctures. Figure 8 shows that this expectation is borne out for one of the interactions but not for the other. This probably means that the energy difference is not very great, and the near identity of the ball/porphyrin plane separations would seem to support this. On the other hand, there are crystal packing considerations and, of course, the functionalized C₆₀ moieties are not free to rotate. These features of the solid state may prevent the buckyballs from adopting their truly optimal orientation with respect to the porphyrin.

The binding of fullerenes to tetraphenylporphyrin moieties is believed to be the basis by which chromatographic separation of fullerenes is achieved with a porphyrin-modified silica gel column.²⁹ Indeed, the graphical representation envisaged by Meyerhoff and co-

(23) Meidine, M. F.; Hitchcock, P. B.; Kroto, H. W.; Taylor, R.; Walton, D. R. M. *J. Chem. Soc., Chem. Commun.* **1992**, 1534–1537.
(24) Crane, J. D.; Hitchcock, P. B.; Kroto, H. W.; Taylor, R.; Walton, D. R. M. *J. Chem. Soc., Chem. Commun.* **1992**, 1764–1765.

(25) (a) The shortest known arene–C₆₀ interaction is 2.94 Å in C₆₀-hexamethylbenzene (Sun, Y.-P.; Drovetskaya, T.; Reed, C. A. Unpublished results). In this structure, C₆Me₆ is sandwiched between C₆₀ molecules which are separated by a center-to-center distance of 12.96 Å. The C···C diameter of C₆₀ is taken as 7.08 Å.^{24,25g} (b) Ermer, O. *Helv. Chim. Acta* **1991**, 74, 1339–1351. (c) Balch, A. L.; Catalano, V. J.; Lee, J. W.; Olmstead, M. M. *J. Am. Chem. Soc.* **1992**, 114, 5455–5457. (d) Chiang, L. Y.; Swirczewski, J. W.; Liang, K.; Millar, J. *Chem. Lett.* **1994**, 981–984. (e) Osterodt, J.; Nieger, M.; Vögtle, F. *J. Chem. Soc., Chem. Commun.* **1994**, 1609–1608. (f) Steed, J. W.; Junk, P. C.; Atwood, J. L.; Barnes, M. J.; Raston, C. L. *J. Am. Chem. Soc.* **1994**, 116, 10346–10347. (g) Fedurco, M.; Olmstead, M. M.; Fawcett, W. R. *Inorg. Chem.* **1995**, 34, 390–392. (h) Atwood, J. L.; Barnes, M. J.; Gardiner, M. G.; Raston, C. L. *Chem. Commun.* **1996**, 1449–1450.

(26) Xie, Z.; Bau, R.; Reed, C. A. *Angew. Chem., Int. Ed. Engl.* **1994**, 33, 2433–2434.

(27) Xie, Z.; Reed, C. A. Unpublished results.

(28) The present structure shows partial metalation of the porphyrin with cobalt(II), a residue from the synthesis. Independently, Balch and co-workers have isolated cobalt octaethylporphyrin/fullerene species showing similar close interactions: reported at the Electrochemical Society Meeting, Los Angeles, May 6–10, 1996.

(29) (a) Xiao, J.; Savina, M. R.; Martin, G. B.; Francis, A. H.; Meyerhoff, M. E. *J. Am. Chem. Soc.* **1994**, 116, 9341–9342. (b) Kibbey, C. E.; Savina, M. R.; Parseghian, B. K.; Francis, A. H.; Meyerhoff, M. E. *Anal. Chem.* **1993**, 65, 3717–3719.

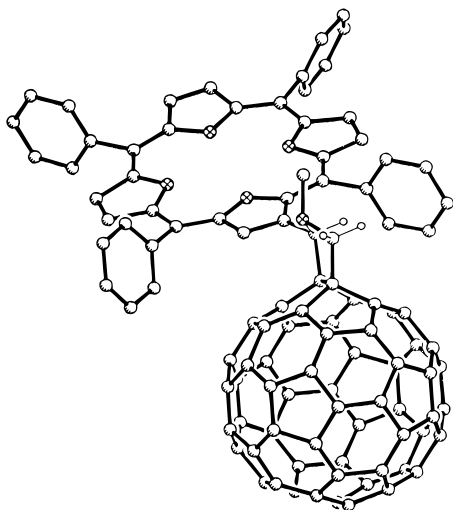


Figure 8. Perspective drawing of **2** showing the addition across a 6:6 ring juncture and a trans (equatorial–equatorial) disposition of the methyl and porphyrin substituents with respect to the C–N bond of the pyrrolidine ring.

workers for the interaction of C_{60} with zinc tetraphenylporphyrin (see Figure 3 in ref 29a) is remarkably close to that observed in the present work. They emphasize π/π interactions, overall fullerene basicity, and shape selectivity as important factors in understanding the chemical basis of the chromatographic discrimination mechanism. The present work suggests that a fairly specific donor/acceptor interaction is of major importance. In particular, the retention differences between fullerenes and endohedral metallofullerenes, which have dipole moments, can be readily understood in terms of a donor/acceptor relationship.

Despite the widespread use of pyrrolidine functionalization of C_{60} , this is the first pyrrolidine derivative to be characterized by X-ray crystallography. It confirms that the azamethine ylide addition occurs across a 6:6 ring juncture, as previously deduced from ^{13}C NMR spectroscopy.¹¹ Two further, more subtle aspects of bond connectivity and conformation are revealed by this structure. The first concerns isomer preference in 2-substituted pyrrolidines. There are cis and trans dispositions possible for the *N*-methyl and 2-porphyrin substituents on the C–N bond of the five-membered pyrrolidine ring. As shown in Figure 8, the X-ray structure reveals the trans disposition. This indicates a substantial bias toward trans addition in the synthetic reaction^{3b} because the material used in this work is the major product. A minor product was observed in the chromatographic purification. Its 1H NMR spectrum is consistent with a nonequilibrating cis isomer, but there was insufficient material to achieve a complete characterization. The second aspect concerns the conformational preference of the *N*-methyl substituent. Inspection of Figure 8 reveals its equatorial orientation, i.e., the lone pair on the N atom is axial. This is consistent with data on other *N*-methylpyrrolidines whose structures have been determined by X-ray crystallography³⁰ and with the result of

a molecular mechanics calculation.³¹ The equatorial/axial preference in this calculation, however, was only 1 kcal and was reversed in a semiempirical calculation.¹⁹ This suggests that the equatorial substituent preference is real, but not particularly strong.

Chromophore/Chromophore Interactions. Compounds **2**, **3**, and **4** provide opportunities to observe the perturbation of the electronic structure of a functionalized C_{60} moiety by a nearby porphyrin or C_{60} chromophore. Since each of these species has the same pyrrolidine functionality, direct comparisons can be made to **1**. As the connectivities in **2–4** involve sp^3 carbon linkages to remote chromophores, the mutual influence of the chromophores will be largely through space, at van der Waals, or solvent-separated contact. Our studies have been directed at ground state electronic perturbation,^{3b} excited state phenomena,⁸ redox potential influences,⁸ and, now, spin coupling effects.

The ground state perturbation of the NIR spectrum of the C_{60}^{1-} moiety is indicated by shifts from λ_{max} in **1**¹⁻ where it is 1002 nm. The shift is to higher energy for the porphyrin species and increases from Cu(II)-metalated **2** (993 nm) to free base **2** (986 nm) in *o*-dichlorobenzene solution. The shift is to lower energy in **3** and **4** by the same amount (to 1015 nm) in benzonitrile solution. These effects are relatively small and probably reflect the proximity and solvation influences of the appendage. The same is true for the redox potentials of **2**, **3**, and **4**. Under identical conditions (benzonitrile, $Bu_4N^+PF_6^-$), the three reduction waves of **1** are shifted by no more than 20 mV in **2**,⁸ **3**, and **4**.

Spin coupling effects were investigated in Cu(II)-metalated **2**¹⁻, but no significant evidence of coupling was found. The EPR spectrum of **2**¹⁻ was essentially the same as that of **1**¹⁻. The EPR spectrum of Cu(II)-metalated **2**¹⁻ was essentially the summation of **2**¹⁻ and Cu(II)-metalated **2**. This can be understood in terms of the nature of the magnetic orbitals. The Cu(II) unpaired electron is in a $d_{x^2-y^2}$ orbital and would be delocalized into the σ^*_{Cu-N} orbitals of the porphyrin. On the other hand, the unpaired electron on the C_{60}^{1-} moiety is in a π^* orbital. These orbitals are not cospatial via van der Waals contact, nor do they interact via the pyrrolidine linkage. This contrasts with the UV–vis and NIR mutual perturbations of electronic spectra where π/π van der Waals effects are observed.

The most interesting spin coupling effect is observed in **3**²⁻ where two C_{60}^{1-} moieties are held in van der Waals contact by virtue of the 1,3-phthalamido linkage. As shown in Figure 9, triplet “wings” ($\Delta H = 29$ G) are evident in **3**²⁻ in addition to the dominant central doublet of spin-isolated C_{60}^{1-} moieties. These triplet features are absent in **1**¹⁻, **2**¹⁻, **3**¹⁻, and **4**¹⁻ and essentially absent in **4**²⁻. We believe that the triplet arises from intramolecular ball-to-ball spin–spin interactions. An investigation of possible conformations of the neutral form of **3** using molecular mechanics³¹ has found that the most stable structure, by more than 10 kcal/mol, is that with the two balls in near van der Waals contact. The enhanced stability of this conformation for this model arises from

(30) (a) Murray-Rust, P.; Murray-Rust, J.; Middlemiss, D. *Acta Crystallogr. B* **1980**, *36* 1678–1680. (b) Greco, M. N.; Rasmussen, C. R. *J. Org. Chem.* **1992**, *57*, 5532–5535. (c) Tetzlaff, C.; Butz, V.; Vilsmaier, E.; Wagemann, R.; Maas, G.; Ritter von Onciul, A.; Clark, T. *J. Chem. Soc., Perkin Trans. 2* **1993**, 1901–1905. (d) Seibel, J.; Vilsmaier, E.; Fröhlich, K.; Maas, G.; Wagemann, R. *Tetrahedron* **1994**, *50*, 715–730.

(31) Calculations were performed using Cerius 2, BIOSYM/Molecular Simulations, San Diego, CA. The model employed the Universal Force Field³² with the Charge Equilibration method.³³

(32) Rappé, A. K.; Casewit, C. J.; Colwell, K. S.; Goddard, W. A.; Skiff, W. M. *J. Am. Chem. Soc.* **1992**, *114*, 10024–10035.

(33) Rappé, A. K.; Goddard, W. A. *J. Phys. Chem.* **1991**, *95*, 3358–3363.

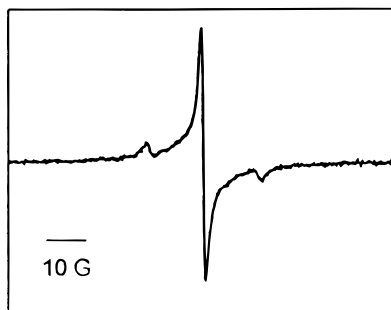


Figure 9. Frozen solution EPR spectra of 3^{2-} at 83 K showing central doublet features ($g = 2.0006$, $\Delta H = 1.1$ G) and triplet "wings" ($\Delta H = 29$ G, $g = 2.0007$).

an attractive van der Waals interaction between the balls of about 10 kcal. The close proximity of the two balls (nearest C–C contact 3.2 Å) in 3^{2-} should give rise to a magnetic dipole/dipole interaction between the neighboring unpaired spins. The magnitude of the dipolar interaction is reflected in the size of the zero field splitting of the triplet state spectrum, $D = 29$ G (Figure 9). Occasionally, these triplet features are observed at high spectrometer gain settings in species other than 3^{2-} , such as 4^{2-} ; we take this to mean that aggregation effects can, under certain circumstances, bring about small amounts of intermolecular spin–spin interaction. This observation may be important in understanding the bulk ferromagnetism observed in $[\text{TDAE}^+][\text{C}_{60}^{1-}]$.³⁴

On the Origin of "Spurious" EPR Signals in C_{60}^{n-} . As discussed earlier, the EPR signals of pyrrolidine-functionalized C_{60}^{1-} moieties are characterized by sharp doublets with g values less than the free electron value, and line widths of about 1 G that are not particularly temperature dependent. This line width behavior contrasts markedly with the predominant EPR signal of C_{60}^{1-} which, in most reports, increases from several gauss at low temperature to tens of gauss at room temperature. The features of the pyrrolidine-functionalized C_{60}^{1-} moieties are, however, very similar to the minor signal or "spike" in the EPR spectrum of C_{60}^{1-} . This minor signal has been variously ascribed to ion pairing effects, disproportionation, a thermally accessible excited state,

(34) (a) Allemand, P.-M.; Khemani, K. C.; Koch, A.; Holczer, K.; Donovan, S.; Gruner, G.; Thompson, J. D.; Wudl, F. *Science* **1991**, *253*, 301–303. (b) Gotschy, B *Phys. Rev. B* **1995**, *52*, 7378–7383.

impurities, or aggregation effects.¹⁴ The present work supports the notion that the presence of a functionalized fulleride(1^-) as a minor impurity in C_{60} could give rise to the minor EPR signal in C_{60}^{1-} . On the other hand, it is hard to believe that everyone's C_{60} is contaminated with similar amounts of a functionalized impurity that gives a sharp EPR signal when reduced.³⁵

Conclusion

Upon reduction to the fulleride(1^-) state, monofunctionalized C_{60} retains much of its parent C_{60}^{1-} character. The frontier electronic levels have lower symmetry, and the LUMO is typically shifted to somewhat higher energy but the delocalized π character is retained. The interaction of functionalized C_{60} with itself or with other chromophores via this π system shows considerable potential in applications to problems of electron transfer³⁶ and spin coupling. Although the data in the present work were gathered on pyrrolidine-functionalized species, it seems likely that the observed features will be seen in other monofunctionalized C_{60} derivatives. It remains to be seen what the range and extent of these features will be since presently available data are limited mainly to reduction potential measurements and ground state UV–vis spectral perturbations.

Acknowledgment. We thank Dr. Zuwei Xie for help with the X-ray structure determination and the National Institutes of Health (GM 23851 to C.A.R.) and the Marsden Fund of New Zealand (UOA613 to P.D.W.B.) for support.

JO970357U

(35) The observation of triplet features from the side-by-side 1^- buckyballs in 3^{2-} has led us to entertain the notion that dimers are responsible for the observation of minor EPR signals in C_{60}^{n-} . Interestingly, the 29 G splitting in 3^{2-} corresponds exactly to the perpendicular portion of the "high temperature triplet" ($2D = 58$ G) seen as a minor signal in the EPR spectrum of C_{60}^{2-} .^{14c} In both cases, the signals are not observable at 4K and their g values are very similar (ca. 2.0005). This raises the possibility that aggregation of C_{60}^{2-} leads to a range of disproportionation products, one of which may be $(\text{C}_{60})_2^{2-}$. Whether such species have a specific, weak C–C bond is very difficult to say. More experiments on this tricky problem are needed.

(36) Yu, G.; Gao, J.; Hummelen, J. C.; Wudl, F.; Heeger, A. J. *Science* **1995**, *270*, 1789–1791.

(37) The author has deposited atomic coordinates for this structure with the Cambridge Crystallographic Data Centre. The coordinates can be obtained, on request, from the Director, Cambridge Crystallographic Data Centre, 12 Union Road, Cambridge, CB2 1EZ, UK.